Brazilian Journal
of Chemical
Engineering

ISSN 0104-6632
Printed in Brazil
www.abeq.org.br/bjche

Vol. 30, No. 01, pp. 13 - 21, January - March, 2013

EQUILIBRIUM AND THERMODYNAMICS OF AZO DYES BIOSORPTION ONTO *Spirulina platensis*

G. L. Dotto, M. L. G. Vieira, V. M. Esquerdo and L. A. A. Pinto*

Unit Operation Laboratory, School of Chemistry and Food, Phone: + (55) (53) 3233 8648,
Fax: + (55) (53) 3233 8745, Federal University of Rio Grande, FURG,
475 Engenheiro Alfredo Huch Street, 96203-900, Rio Grande - RS, Brazil.
E-mail: dqmpinto@furg.br

(Submitted: December 15, 2011 ; Revised: May 23, 2012 ; Accepted: May 23, 2012)

Abstract - The equilibrium and thermodynamics of azo dye (tartrazine and allura red) biosorption onto *Spirulina platensis* biomass were investigated. The equilibrium curves were obtained at 298, 308, 318 and 328 K, and four isotherm models were fitted the experimental data. Biosorption thermodynamic parameters (ΔG, ΔH and ΔS) were estimated. The results showed that the biosorption was favored by a temperature decrease. For both dyes, the Sips model was the best to represent the equilibrium experimental data (R^2>0.99 and ARE<5.0%) and the maximum biosorption capacities were 363.2 and 468.7 mg g^{-1} for tartrazine and allura red, respectively, obtained at 298 K. The negative values of ΔG and ΔH showed that the biosorption of both dyes was spontaneous, favorable and exothermic. The positive values of ΔS suggested that the system disorder increases during the biosorption process.
Keywords: Biosorption; *Spirulina platensis*; Azo dyes.

INTRODUCTION

More than 0.7 million tons of synthetic organic dyes are produced annually worldwide (Koprivanac and Kusic, 2009). Azo dyes make up approximately 70% of all dyes used worldwide by weight. They are extensively used in the textile, paper, food, leather, cosmetics and pharmaceutical industries (Saratale *et al*., 2011). Discharge of these dyes in effluents affects aquatic plants because they reduce sunlight transmission through water. Also azo dyes may impart toxicity to aquatic life and may be mutagenic, carcinogenic and may cause severe damage to human beings, such as dysfunction of the kidneys, reproductive system, liver, brain and central nervous system (Salleh *et al*., 2011). Thus, several governments have established environmental restrictions with regard to the quality of colored wastewater and have forced dye-using industries to remove dyes from their effluents before discharging (Mahmoodi *et al*., 2010). The conventional methods are generally ineffective in color removal, and they are expensive and less adaptable to a wide range of dye wastewaters (Srinivasan and Viraraghavan, 2010). In this way, biosorption is an alternative eco-friendly technology for removal of azo dyes from aqueous solutions, due its simplicity of design, ease of operation, insensitivity to toxic substances and complete removal of pollutants, even from dilute solutions (Aksu, 2005).

Biosorption is the passive uptake of pollutants from aqueous solutions by the use of non-growing or dead microbial biomass, thus allowing the recovery and/or environmentally acceptable disposal of the pollutants (Aksu, 2005). Many biosorbents have been used to remove dyes from aqueous solutions, such as, *Chlorella vulgaris* (Aksu and Tezer, 2005), *Azolla rongpong* (Padmesh *et al*., 2006), *Aspergillus foetidus* (Patel and Suresh, 2008), *Aspergillus parasiticus* (Akar *et al*., 2009), *Ulothrix* sp. (Dogar *et al*., 2010) and *Nostoc linckia* (Mona *et al*., 2011), but studies about the use of *S. platensis* are very

*To whom correspondence should be addressed
This article is an extended version of a work presented at CBTermo-2011 - VI Brazilian Congress of Applied Thermodynamics 2011, Salvador, Bahia, Brasil.

limited. *S. platensis*, a member of blue-green algae, contains a variety of functional groups such as carboxyl, hydroxyl, sulfate, amine, phosphate and other charged groups on the surface, which can sequester pollutants (Seker *et al*., 2008). This microalgae was successfully employed for removal of chromium, cadmium, cooper, lead and nickel from aqueous solutions (Chojnacka *et al*., 2005; Seker *et al*., 2008). However, its use to remove dyes is rarely investigated.

The equilibrium and thermodynamic analysis of the biosorption process is fundamental in order to obtain information about the interactions adsorbate-biosorbent, and so increase the process efficiency (Aksu, 2005). The equilibrium curve (isotherms) leads to information about the biosorption mechanism and also about the maximum biosorption capacity (Blázquez *et al*., 2010). The shape of an isotherm not only provides information on the biosorption affinity of dye molecules, but also reflects thermodynamic data, leading to relevant information about biosorption spontaneity and the stability of the biosorbent-adsorbate interactions (Aksu, 2005; Piccin *et al*., 2011; Dotto *et al*., 2011).

In this work, the equilibrium and thermodynamics of azo dye (tartrazine and allura red) biosorption onto *S. platensis* biomass in batch systems were studied. Temperature effect on the experimental equilibrium curves was verified, and the Langmuir, Freundlich, Dubinin-Radushkevich and Sips models were fitted to the experimental data. The values of the Gibbs free energy change (ΔG), enthalpy change (ΔH) and entropy change (ΔS) for the biosorption process were estimated.

MATERIALS AND METHODS

Preparation and Characterization of *Spirulina platensis*

S. platensis strain LEB-52 was cultivated in a 450 L open outdoor photo-bioreactor, under uncontrolled conditions, in the south of Brazil. During these cultivations, water was supplemented with 20% Zarrouk synthetic medium (Costa *et al*., 2004). At the end of cultivation, the biomass was recovered by filtration, washed with distilled water and pressed to recover the biomass with a moisture content of 76% (wet basis).

The wet biomass (cylindrical pellet form with a diameter of 3 mm) was dried in perforated trays using perpendicular air flow. The drying conditions were: air temperature 60 °C, air velocity 1.5 m s^{-1}, relative humidity between 7% and 10%, load in tray 4 kg m^{-2} (Oliveira *et al*., 2009). The dried biomass was ground in a mill (Wiley Mill Standard, No. 03, USA) and sieved until the discrete particle size ranged from 68 to 75 μm.

The particles were characterized according to the centesimal chemical composition (AOAC, 1995) and point of zero charge (pH_{zpc}) using the eleven points experiment (Hao *et al*., 2004). The functional groups of the *S. platensis* biomass were identified using infra-red analysis (FT-IR) (Prestige 21, the 210045, Japan) (Mona *et al*., 2011). The specific surface area, pore volume and average pore radius were determined by standard BET N_2-adsorption methods (Quantachrome, Nova station A, USA) (Schimmel *et al*., 2010). Scanning electron microscopy (SEM) was used to verify the surface characteristics of the *S. platensis* particles (Jeol, JSM-6060, Japan) (Bangash and Alan, 2009). The samples were sputter-coated with a thin conductive layer of gold for 400 s, and images were then obtained using an acceleration voltage of 10 kV with magnification ranging from 300 to 2000 fold. The thermal profile of the *S. platensis* particles was obtained in a N_2 atmosphere using TG and DTG curves (PG instruments, SDT Q600, U.K.) (Gottipati and Mishra, 2010).

Adsorbate

In this work, the azo dyes tartrazine (molecular weight 534.4 g mol^{-1}, purity 85%, color index 19140, maximum wavelength 425 nm, pKa = 9.4) and allura red (molecular weight 496.4 g mol^{-1}, purity 85%, color index 16045, maximum wavelength 500 nm, pKa = 11.4) (Pluryquímica Ltda., Brazil) were employed for the batch experiments. Distilled water was used to prepare all solutions. The chemical structures of the dyes are illustrated in Figure 1.

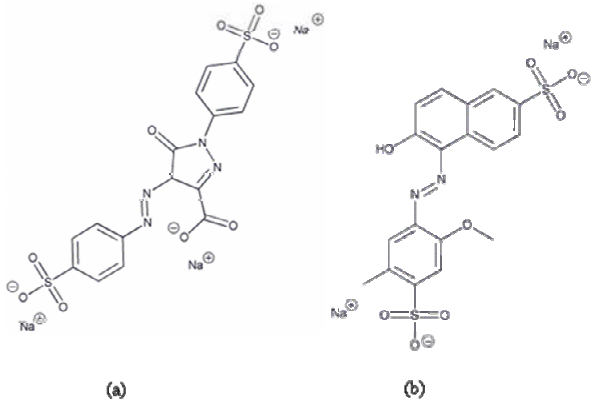

Figure 1: Chemical structures of the azo dyes: (a) tartrazine and (b) allura red.

Batch Equilibrium Experiments

The equilibrium biosorption isotherms were determined using batch studies under different temperature conditions (298, 308, 318 and 328 K). *S. platensis* particles (50 mg dry basis) were added to 90 mL of distilled water. The pH of the suspension was corrected (pH = 4) through addition of 10 mL of disodium phosphate/ citric acid buffer solution (0.1 mol L^{-1}), which did not present interaction with the dyes. The suspension was agitated at 10000 rpm (Dremel, 1100-01, Brazil) for 5 min. Different volumes of the dye stock solution containing 10 g L^{-1} were added to the *S. platensis* suspensions and adjusted to 200 mL with distilled water. The suspensions were placed in flasks and agitated at 100 rpm using a thermostated Wagner type agitator (FANEM, 315 SE, Brazil). Samples were analyzed every 8 h. The equilibrium was attained when the dye concentration in the liquid did not change between three consecutive measurements. The biomass and biosorbed dyes were removed from the liquid by filtration through Whatmann No. 40 Filter Paper, which did not present interaction with the dyes, and the dye concentration was determined by spectrophotometry (Quimis, Q108, Brazil) (Aksu and Tezer, 2005; Piccin *et al*., 2009; Dotto and Pinto, 2011a; Dotto and Pinto 2011b). The experiments were carried out in replicate (three times for each experiment) and blanks were performed.

The biosorption capacity at equilibrium (q_e), valid when the solute remaining in the liquid filling the pores is negligible, was determined according to Equation (1):

$$q_e = \frac{C_0 - C_e}{m} V \tag{1}$$

where C_0 is the initial dye concentration in the liquid phase (mg L^{-1}), C_e is the dye concentration in the liquid phase at equilibrium (mg L^{-1}), m is the biosorbent amount (g) and V is the volume of suspension (L).

Equilibrium Isotherm Models

The biosorption equilibrium data, commonly known as biosorption isotherms, describe how pollutants interact with biosorbent materials and so are critical for optimizing the use of biosorbents (Aksu, 2005). This manner is very important to obtain a model that represents the experimental equilibrium data. In this work, Langmuir, Freundlich, Dubinin-Radushkevich and Sips models were fitted to the experimental data.

The Langmuir isotherm is derived by assuming a uniform surface with finite identical sites and mono-layer adsorption of the adsorbate (Langmuir, 1916). The Langmuir isotherm is shown in Equation (2):

$$q_e = \frac{q_m k_L C_e}{1 + k_L C_e} \tag{2}$$

where q_m is the maximum monolayer biosorption (mg g^{-1}) and k_L is the Langmuir constant (L mg^{-1}).

Another essential characteristic of the Langmuir isotherm can be expressed by the separation factor or equilibrium factor (R_L) (Langmuir, 1916), as demonstrated in Equation (3):

$$R_L = \frac{1}{1 + k_L C_0} \tag{3}$$

The Freundlich adsorption isotherm gives the empirical relation between q_e and C_e (Freundlich, 1906). The Freundlich isotherm is given by Equation (4):

$$q_e = k_F C_e^{1/n} \tag{4}$$

where k_F is the Freundlich constant ((mg g^{-1}) (mg $L^{-1})^{-1/n}$) and 'n' is the biosorption intensity.

Another equation used in the analysis of isotherms was proposed by Dubinin and Radushkevich (1947), and can be represented by Equation (5):

$$q_e = q_S \exp(-B\varepsilon^2) \tag{5}$$

where q_s is the D–R constant (mg g^{-1}) and ε can be correlated according to Equation (6):

$$\varepsilon = RT\ln\left(1 + \frac{1}{C_e}\right) \tag{6}$$

The constant B (mol^2 kJ^{-2}) gives the mean free energy E (kJ mol^{-1}) of adsorption per molecule of adsorbate when it is transferred to the surface of the solid from infinity in the solution (Dubinin and Radushkevich, 1947), and can be computed using Equation (7):

$$E = \frac{1}{\sqrt{2B}} \tag{7}$$

The Sips isotherm is a combination of the Langmuir and Freundlich isotherms (Sips, 1948), as

demonstrated in Equation (8):

$$q_e = \frac{q_{ms}(k_S C_e)^{ms}}{1+(k_S C_e)^{ms}} \quad (8)$$

where q_{ms} is Sips maximum biosorption capacity (mg g^{-1}), k_S is the Sips constant (L mg^{-1}) and ms the exponent of the Sips model.

The isotherm parameters were determined by nonlinear regression, using the software Statistica 6.0 (Statsoft, USA.). The fit quality was measured according to the coefficient of determination (R^2) and average relative error (ARE) (Piccin *et al*., 2009).

Biosorption Thermodynamics

The values of ΔG, ΔH and ΔS are important information in order to elucidate the biosorption thermodynamic behavior (Aksu, 2005). In this work, the values of Gibbs free energy change (ΔG), enthalpy change (ΔH) and entropy change (ΔS) were estimated using Equations (9) and (10) as demonstrated by Milonjic, (2007):

$$\Delta G = -RT\ln(\rho K_D) \quad (9)$$

$$\ln(\rho K_D) = -\frac{\Delta H}{RT} + \frac{\Delta S}{R} \quad (10)$$

where, R is the universal gas constant (8.314 J mol^{-1} K^{-1}), T is the temperature (K), K_D is the thermodynamic equilibrium constant (L g^{-1}) and ρ is the water density (g L^{-1}). The K_D values were estimated from the parameters of the best fit isotherm model.

RESULTS AND DISCUSSION

Spirulina platensis Characterization

The percentage chemical composition of *S. platensis* used in the biosorption tests is shown in Table 1.

The values presented in Table 1 are similar to the percentage chemical composition obtained by Oliveira *et al*. (2009) and show that *S. platensis* is composed of several biomolecules. According to Chojnacka *et al*. (2005), these biomolecules contain functional groups which can sequester pollutants. The functional groups of *S. platensis* were identified by FT-IR as shown in Figure 2.

Table 1: Percentage chemical composition of *Spirulina platensis*.

Chemical composition (wet basis)*	
Moisture content (%) w.b.)	9.7±0.5
Ash (%)	6.3±0.2
Protein (%)	67.0±0.7
Lipids (%)	7.0±0.1
Carbohydrate (%)	10.0±0.5

*mean value ± standard error (n=3).

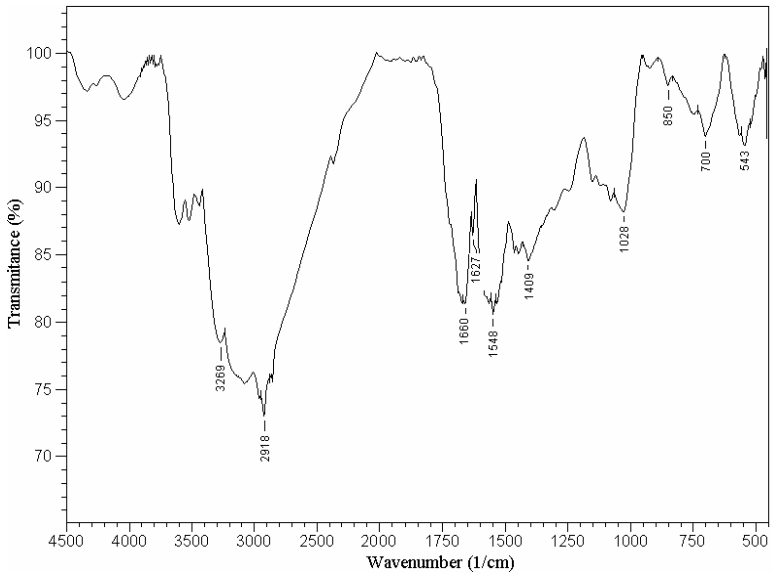

Figure 2: FT-IR spectrum of *Spirulina platensis*.

In Figure 2 the major intense bands were around 3269, 2918, 1660, 1627, 1548, 1409, 1028, 850, 700 and 543 cm^{-1}. The O-H bond stretching mixed with NH_2 group can be observed at 3269 cm^{-1}. The peak 2918 cm^{-1} is relative to CH_2 stretching. The scissor bending of NH_2 groups can be observed at 1660 cm^{-1}. At 1627 and 1548 cm^{-1} C=C stretching can be observed. The bands at 1409 and 1028 cm^{-1} could be attributed to –S–O and –P–O, respectively. The band of 850 cm^{-1} could be attributed to an N-H stretch of amide or amine. The adsorption peaks in the region 700 cm^{-1} could be attributed to aromatic –CH bending vibrations. At 1543 cm^{-1} R-S-O can be observed. These functional groups may be responsible for dye binding (Aksu, 2005; Chojnacka *et al*., 2005; Seker *et al*., 2008).

The values of zero point charge (pH_{zpc}), specific surface area, pore volume and average pore radius of the biosorbent are very important to understand the biosorption mechanisms (Schimmel *et al*., 2010). The zero point charge (pHzpc) of the *S. platensis* biomass (obtained by the eleven point's experiment) was 7, showing that when the pH of the suspension is lower than 7, the surface of the *S. platensis* biomass is positively charged (Hao *et al*., 2004). *S. platensis* particles presented specific surface area of 3.5 $m^2\ g^{-1}$, pore volume of 3.9 $mm^3\ g^{-1}$and average pore radius of 22.5Å.

Scanning electron microscopy (SEM) was carried out in order to verify the surface characteristics of *S. platensis* particles. Figure 3 shows SEM images of *S. platensis*: (a) distributed particles and (b) particle surface.

It was observed in Figure 3 (a) that the *S. platensis* particles presented different forms and mean diameter in the range from 68 to 75 μm. In Figure 3 (b) a rough and homogeneous surface was observed. In addition, in Figures 3 (a) and (b), the rigid and non-porous structure of the *S. platensis* particles can be observed.

To verify the thermal profile of the *S. platensis* particles used in the biosorption experiments, TG and DTG curves were used. TG and DTG curves of *S. platensis* particles are shown in Figure 4.

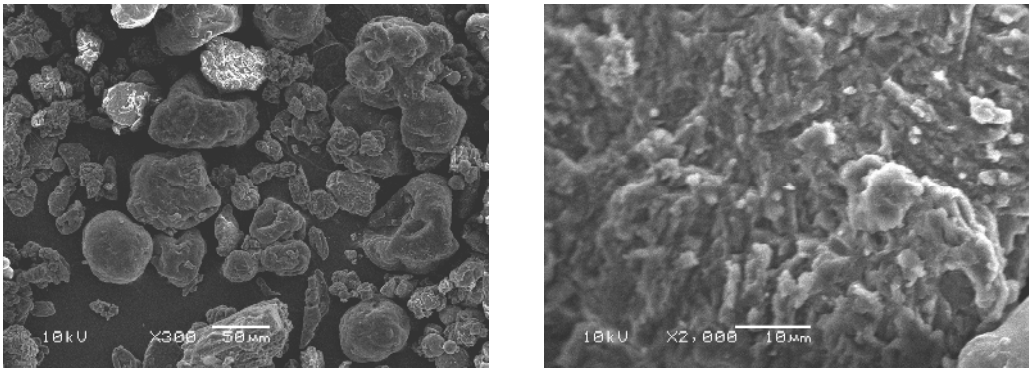

(a) (b)

Figure 3: SEM images of *Spirulina platensis*: (a) distributed particles and (b) particle surface.

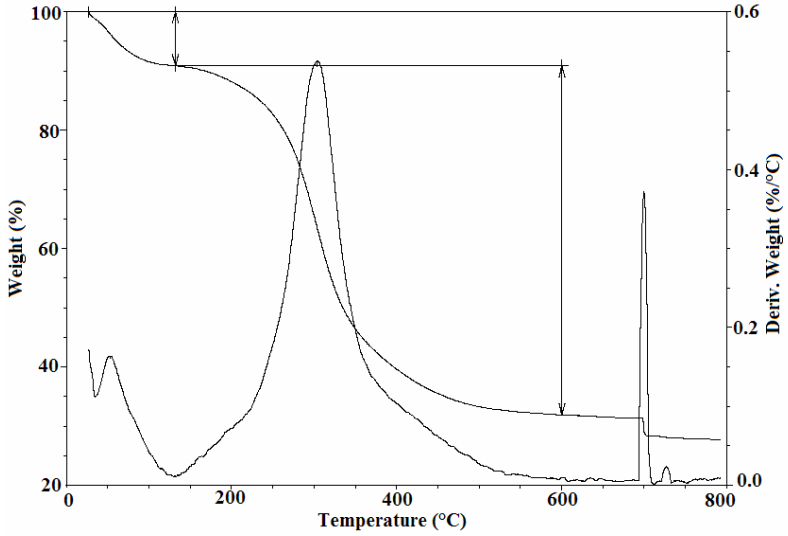

Figure 4: TG and DTG curves of *Spirulina platensis* particles.

TG and DTG curves demonstrate that *S. platensis* particle mass loss occurred in three steps. The first mass loss step, from about 25 °C to 140 °C concerns the loss of water, which is adsorbed on the *S. platensis* particles. The decomposition of the *S. platensis* particles is observed from about 150 °C to 500 °C. A carbonization of material was observed up to 500 °C. This shows that, under experimental conditions of biosorption, *S. platensis* particles maintained their physical characteristics.

Biosorption Isotherms

The equilibrium experimental curves of azo dye biosorption onto *S. platensis* particles at different temperatures (298, 308, 318, 328 K) are presented in Figure 5 (a) tartrazine and (b) allura red.

The biosorption isotherms of tartrazine (Figure 5 (a)), were characterized by an initial step of weak attraction between *S. platensis* and the dye, followed by a strong increase in the biosorption capacity, and finally a plateau was observed. According to Blázquez *et al*. (2010), this behavior is common for a type "V" isotherm. On the other hand, in the allura red biosorption isotherms (Figure 5 (b)), the equilibrium curves presented an initial step of increase in biosorption capacity followed by a plateau. In this case, type "I" isotherms were observed. These results suggested that allura red biosorption onto *S. platensis* particles occurred by formation of a monolayer. However, for tartrazine, biosorption occurred by formation of a multilayer.

It can be observed in Figure 5, for both tartrazine and allura red, that a temperature decrease caused an increase in biosorption capacity, the best results being obtained at 298 K. This behavior can be explained by two main aspects: Firstly, the temperature increase causes an increase in the solubility of the dyes (Koprivanac and Kusic, 2009) so, the interaction forces between the dyes and the solvent become stronger than those between dyes and *S. platensis* particles. Coupled to this, according to Aksu (2005), at temperatures above 318 K damage of sites on the surface of biomass can occurs and, consequently, a decrease in the surface activity. Piccin *et al*. (2011) showed that the temperature increase caused a decrease in the adsorption capacity of FD&C red n° 40 onto chitosan. Similar behavior was obtained by Aksu and Tezer (2005) in the biosorption of remazol red and remazol golden yellow using *Chlorella vulgaris* as biosorbent. They obtained best results at 298 K.

In order to obtain an equation to represent the equilibrium experimental data, Langmuir, Freundlich, Dubinin-Radushkevich and Sips models were fitted to the experimental data. The isotherm parameters, their respective coefficients of determination (R^2) and average relative error (ARE) values are shown in Table 2.

It was observed in Table 2 for biosorption of tartrazine onto *S. platensis* particles, that Dubinin-Radushkevich and Sips isotherms presented high values of the coefficient of determination (R^2>0.95), indicating a good fit to the experimental data. However, the D-R model presented high values of the average relative error (ARE>14%), consequently, overestimating the maximum biosorption capacity values. Thus, the Sips model was the best to represent the equilibrium experimental data (R^2>0.98 and ARE<5%). In the case of allura red biosorption, the Langmuir and Sips models presented high values of the coefficient of determination and low values of the average relative error (R^2>0.99 and ARE<3%), but the Sips model was more appropriate because it estimated more accurately the maximum biosorption capacity values.

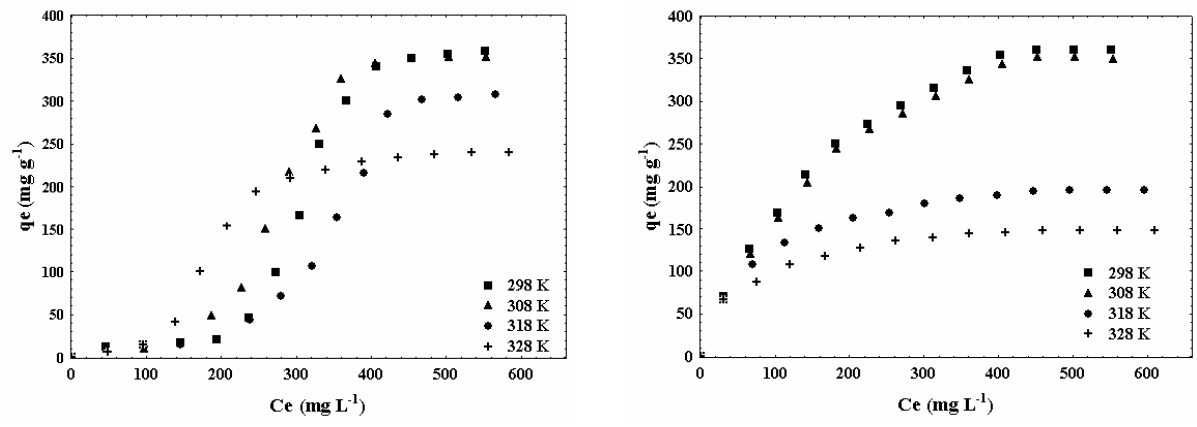

Figure 5: Biosorption equilibrium isotherms of (a) Tartrazine and (b) Allura red: ■ T=298 K; ▲ T=308 K; ● T=318 K; + T=328 K.

Table 2: Isotherm parameters of azo dye biosorption by *Spirulina platensis*.

Models	Tartrazine				Allura red			
	298 K	308 K	318 K	328 K	298 K	308 K	318 K	328 K
Langmuir								
q_m (mg g^{-1})	3299.5	3142.5	3305.6	598.5	503.4	499.2	225.2	164.1
$k_L x10^3$ (L mg^{-1})	0.22	0.24	0.16	1.42	5.28	4.95	12.91	16.99
R_L	0.87	0.86	0.91	0.52	0.26	0.27	0.12	0.10
R^2	0.81	0.86	0.80	0.89	0.99	0.99	0.99	0.99
ARE (%)	142.7	131.6	129.3	79.8	1.7	2.1	0.8	2.6
Freundlich								
k_F((mg g^{-1}) (L $mg^{-1})^{1/n}$)	0.02	0.13	0.01	2.20	20.35	18.41	31.76	31.96
N	0.64	0.79	0.60	1.39	2.13	2.08	3.38	4.02
R^2	0.89	0.89	0.92	0.87	0.97	0.97	0.97	0.98
ARE (%)	65.6	79.8	46.2	85.5	7.9	8.2	5.6	4.3
Dubinin-Radushkevich								
q_s (mg g^{-1})	568.9	492.5	528.2	273.0	348.0	340.11	182.65	137.81
B (mol^2 kJ^{-2})	0.093	0.059	0.107	0.020	0.006	0.006	0.002	0.001
E (kJ mol^{-1})	2.3	2.9	2.1	5.0	9.1	8.9	19.6	26.7
R^2	0.96	0.97	0.97	0.98	0.88	0.88	0.80	0.71
ARE (%)	18.4	18.9	23.4	14.8	15.9	15.8	15.9	19.3
Sips								
q_{ms} (mg g^{-1})	363.2	362.9	334.6	238.2	468.7	454.1	227.1	180.9
k_S (L mg^{-1})	0.0033	0.0032	0.0029	0.0034	0.0061	0.0060	0.0117	0.0139
m_S	8.4	6.3	6.4	4.8	1.1	1.1	1.0	0.8
R^2	0.99	0.99	0.99	0.99	0.99	0.99	0.99	0.99
ARE (%)	4.8	2.6	2.1	1.1	2.0	2.2	0.7	2.1

The high values of "ms" from the Sips model (Table 2) confirmed that tartrazine biosorption onto *S. platensis* occurred by formation of a multilayer. On the contrary, the "ms" values for allura red (Table 2) were near to 1, confirming the formation of a monolayer on the *S. platensis* surface. In summary, for both azo dyes, the Sips model was the best to represent the equilibrium experimental data. The maximum biosorption capacities were 363.2 mg g^{-1} and 468.7 mg g^{-1} for tartrazine and allura red, respectively, obtained at 298 K. These values are in accordance with the specific literature (Aksu, 2005; Aksu and Tezer, 2005; Srinivasan and Viraraghavan, 2010).

Biosorption Thermodynamics

The biosorption thermodynamic parameters (ΔG, ΔH and ΔS) were estimated using Equations (9) and (10). The K_D values were estimated from the Sips parameters (k_S and q_{ms}), because this model presented the best fit with the experimental data. The values of ΔG, ΔH and ΔS are shown in Table 3.

The negative values of ΔG presented in Table 3 showed that the biosorption of the azo dyes tartrazine and allura red onto *S. platensis* particles was a spontaneous and favorable process. The negative values of ΔH (Table 3) suggested that the biosorption was exothermic. The positive values of ΔS indicated that the disorder at the solid-liquid interface increased during the biosorption process. However, Table 3 shows that the enthalpy change (ΔH) contributed more than entropy change (ΔS) to obtain negative values of ΔG. This shows that the azo dyes biosorption onto *S. platensis* was an enthalpy-controlled process. Similar thermodynamic parameters were obtained by Aksu and Tezer (2005) in the biosorption of reactive dyes onto *Chlorella vulgaris,* and also by Dotto *et al*. (2011) in the adsorption of acid blue 9 and food yellow 3 onto chitosan.

Table 3: Thermodynamic parameters of azo dye biosorption by *Spirulina platensis*.

Dye	Temperature (K)	ΔG (kJ mol^{-1})	ΔH (kJ mol^{-1})	ΔS (kJ mol^{-1} K^{-1})
Tartrazine	298	-17.5	-10.9	0.02
	308	-18.0		
	318	-18.2		
	328	-18.3		
Allura red	298	-19.7	-3.3	0.05
	308	-20.2		
	318	-20.8		
	328	-21.3		

CONCLUSION

In this study, the azo dye biosorption onto *S. platensis* was investigated at different temperatures,

using the experimental equilibrium curves and the thermodynamic parameters. The experimental equilibrium curves showed that tartrazine biosorption occurred by formation of a multilayer, but for allura red biosorption occurred by formation of a monolayer on the *S. platensis* surface. For both azo dyes a temperature decrease caused an increase in the biosorption capacity. In all conditions, the Sips model was the best to represent the equilibrium experimental data, the maximum biosorption capacities being 363.2 mg g^{-1} and 468.7 mg g^{-1} for tartrazine and allura red, respectively, obtained at 298 K.The values of Gibbs free energy change (ΔG), enthalpy change (ΔH) and entropy change (ΔS) showed that the azo dye biosorption onto *S. platensis* was spontaneous, favorable, and exothermic, and the system disorder increased during the process.

ACKNOWLEDGEMENTS

The authors would like to thank CAPES (Brazilian Agency for Improvement of Graduate Personnel) and CNPq (National Council of Science and Technological Development) for the financial support.

NOMENCLATURE

ARE	Average relative error	%
B	D-R constant	$mol^2\ kJ^{-2}$
C_e	Equilibrium concentration in the liquid phase	mg L^{-1}
C_0	Initial concentration in the liquid phase	mg L^{-1}
E	Mean free energy per molecule of adsorbate	kJ mol^{-1}
k_D	Thermodynamic equilibrium constant	L g^{-1}
k_F	Freundlich constant	$((mg\ g^{-1})(mg\ L^{-1})^{-1/n})$
k_L	Langmuir constant	L mg^{-1}
k_S	Sips constant	L mg^{-1}
m	Biosorbent amount	g
ms	Sips exponent	dimensionless
n	Biosorption intensity	dimensionless
q_e	Biosorption capacity at equilibrium	mg g^{-1}
q_m	Maximum monolayer biosorption	mg g^{-1}
q_{ms}	Sips maximum biosorption capacity	mg g^{-1}
q_s	D-R constant	mg g^{-1}
R	Universal gas constant	8.314 J mol^{-1} K^{-1}
R_L	Separation factor	dimensionless
R^2	Coefficient of determination	dimensionless
T	Temperature	K
V	Volume of suspension	L

Greek Letters

ΔG	Gibbs free energy change	kJ mol^{-1}
ΔH	Enthalpy change	kJ mol^{-1}
ΔS	Entropy change	kJ mol^{-1} K^{-1}
ε	Biosorption potential	dimensionless
ρ	Water density	g L^{-1}

REFERENCES

A.O.A.C., Official Methods of Analysis. Ed. AOAC, Washington D.C. (1995).

Akar, S. T., Akar, T., Çabuk, A., Decolorization of a textile dye, reactive red 198 (RR198), by *Aspergillus parasiticus* fungal biosorbent. Brazilian Journal of Chemical Engineering, 26, 399-405 (2009).

Aksu, Z., Application of biosorption for the removal of organic pollutants: A review. Process Biochemistry, 40, 997-1026 (2005).

Aksu, Z., Tezer, S., Biosorption of reactive dyes on the green alga *Chlorella vulgaris*. Process Biochemistry, 40, 1347-1361 (2005).

Bangash, F. K., Alam, S., Adsorption of acid blue 1on activated carbon produced from the wood of *Ailanthus altissima*. Brazilian Journal of Chemical Engineering, 26, 275-285 (2009).

Blázquez, G., Calero, M., Hernáinz, F., Tenorio, G., Martín-Lara, M. A., Equilibrium biosorption of lead (II) from aqueous solutions by solid waste from olive-oil production. Chemical Engineering Journal, 160, 615-622 (2010).

Chojnacka, K., Chojnacki, A., Gorecka, H., Biosorption of Cr^{3+}, Cd^{2+} and Cu^{2+} ions by blue–green algae Spirulina sp.: Kinetics, equilibrium and the mechanism of the process. Chemosphere, 59, 75-84 (2005).

Costa, J. A. V., Colla, L. M., Duarte, P. F. F., Improving *Spirulina platensis* biomass yield using a fed-batch process. Bioresource Technology, 92, 237-241 (2004).

Dogar, Ç., Gurses, A., Açıkyıldız, M., Ozkan. E., Thermodynamics and kinetic studies of biosorption of a basic dye from aqueous solution using green algae *Ulothrix* sp. Colloids and Surfaces B: Biointerfaces, 76, 279-85 (2010).

Dotto, G. L., Pinto, L. A. A., Adsorption of food dyes acid blue 9 and food yellow 3 onto chitosan: Stirring rate effect in kinetics and mechanism. Journal of Hazardous Materials, 187, 164-170 (2011b).

Dotto, G. L., Pinto, L. A. A., Adsorption of food dyes onto chitosan: Optimization process and kinetic. Carbohydrate Polymers, 84, 231-238 (2011a).

Dotto, G. L., Vieira, M. L. G., Gonçalves, J. O., Pinto, L. A. A., Removal of acid blue 9, food yellow 3 and FD&C yellow n° 5 dyes from aqueous solutions using activated carbon, activated earth, diatomaceous earth, chitin and chitosan: Equilibrium studies and thermodynamic. Química Nova, 34, 1193-1199 (2011).

Dubinin, M. M., Radushkevich, L. V., Equation of the characteristic curve of activated charcoal. Proceedings of the Academy of Sciences, Physical Chemistry Section, U.S.S.R. 55, 331-333 (1947).

Freundlich, H. M. F., Über die adsorption in lösungen. Zournal Physical Chemistry, 57, 385-470 (1906).

Gottipati, R., Mishra, S., Application of biowaste (waste generated in biodiesel plant) as an adsorbent for the removal of hazardous dye – methylene blue – from aqueous phase. Brazilian Journal of Chemical Engineering, 27, 357-367 (2010).

Hao, X., Quach, L., Korah, J., Spieker, W. A., Regalbuto, J. R., The control of platinum impregnation by PZC alteration of oxides and carbon. Journal of Molecular Catalysis A: Chemical, 219, 97-107 (2004).

Koprivanac, N., Kusic, H., Hazardous Organic Pollutants in Colored Wastewaters. New Science Publishers, New York (2009).

Langmuir, I., The constitution and fundamental properties of solids and liquids. Journal of the American Chemical Society, 38, 2221-2295 (1916).

Mahmoodi, N. M., Hayati, B., Arami, M., Textile dye removal from single and ternary systems using date stones: Kinetic, isotherm, and thermodynamic studies. Journal of Chemical and Engineering Data, 55, 4638-4649 (2010).

Milonjic, S. K., A consideration of the correct calculation of thermodynamic parameters of adsorption. Journal of the Serbian Chemical Society, 72, 1363-1367 (2007).

Mona, S., Kaushik, A., Kaushik, C. P., Biosorption of reactive dye by waste biomass of *Nostoc linckia*. Ecological Engineering, 37, 1589-1594 (2011).

Oliveira, E. G., Rosa, G. S., Moraes, M. A., Pinto, L. A. A., Characterization of thin layer drying of *Spirulina platensis* utilizing perpendicular air flow. Bioresource Technology, 100, 1297-1303 (2009).

Padmesh, T. V. N., Vijayaraghavan, K., Sekaran, G., Velan, M., Application of *Azolla rongpong* on biosorption of acid red 88, acid green 3, acid orange 7 and acid blue 15 from synthetic solutions. Chemical Engineering Journal, 122, 55-63 (2006).

Patel, R., Suresh, S., Kinetic and equilibrium studies on the biosorption of reactive black 5 dye by *Aspergillus foetidus*. Bioresource Technology, 99, 51-58 (2008).

Piccin, J. S., Dotto, G. L., Pinto, L. A. A., Adsorption isotherms and thermochemical data of FD&C Red n° 40 binding by chitosan. Brazilian Journal of Chemical Engineering, 28, 295–304 (2011).

Piccin, J. S., Vieira, M. L. G., Gonçalves, J., Dotto, G. L., Pinto, L. A. A., Adsorption of FD&C Red No. 40 by chitosan: Isotherms analysis. Journal of Food Engineering, 95, 16-20 (2009).

Salleh, M. A. M., Mahmoud, D. K., Abdul Karim, W. A. W., Idris, A., Cationic and anionic dye adsorption by agricultural solid wastes: A comprehensive review. Desalination, 280, 1-13 (2011).

Saratale, R. G., Saratale, G. D., Chang, J. S., Govindwar, S. P., Bacterial decolorization and degradation of azo dyes: A review. Journal of the Taiwan Institute of Chemical Engineers, 42, 138-157 (2011).

Schimmel, D., Fagnani, K. C., Santos, J. B. O., Barros, M. A. S. D., Silva, E. A., Adsorption of turquoise blue QG reactive dye on commercial activated carbon in batch reactor: Kinetic and equilibrium studies. Brazilian Journal of Chemical Engineering, 27, 289-298 (2010).

Seker, A., Shahwan, T., Eroglu, A., Yılmaz, S., Demirel, Z., Dalay, M., Equilibrium, thermodynamic and kinetic studies for the biosorption of aqueous lead(II), cadmium(II) and nickel (II) ions on *Spirulina platensis*. Journal of Hazardous Materials, 154, 973-980 (2008).

Sips, R., On the structure of a catalyst surface. Journal of Chemical Physics, 16, 490-495 (1948).

Srinivasan, A., Viraraghavan, T., Decolorization of dye wastewaters by biosorbents: A review. Journal of Environmental Management, 91, 1915-1929 (2010).